Fermi National Accelerator Laboratory

The Three-point Function as a Probe of Models for Large-scale Structure

JOSHUA A. FRIEMAN[1] & ENRIQUE GAZTAÑAGA[1,2]

[1] *NASA/Fermilab Astrophysics Center*
Fermi National Accelerator Laboratory
Batavia, IL 60510-0500, USA

[2] *Department of Astrophysics*
University of Oxford
Oxford, England OX1 3RH

ABSTRACT

We analyze the consequences of models of structure formation for higher-order (n-point) galaxy correlation functions in the mildly non-linear regime. Several variations of the standard $\Omega = 1$ cold dark matter model with scale-invariant primordial perturbations have recently been introduced to obtain more power on large scales, $R_p \sim 20\ h^{-1}$ Mpc, e.g., low-matter-density (non-zero cosmological constant) models, 'tilted' primordial spectra, and scenarios with a mixture of cold and hot dark matter. They also include models with an effective scale-dependent bias, such as the cooperative galaxy formation scenario of Bower, etal. (1993). We show that higher-order (n-point) galaxy correlation functions can provide a useful test of such models and can discriminate between models with true large-scale power in the density field and those where the galaxy power arises from scale-dependent bias: a bias with rapid scale-dependence leads to a dramatic decrease of the hierarchical amplitudes Q_J at large scales, $r \gtrsim R_p$. Current observational constraints on the three-point amplitudes Q_3 and S_3 can place limits on the bias parameter(s) and appear to disfavor, but not yet rule out, the hypothesis that scale-dependent bias is responsible for the extra power observed on large scales.

Subject Headings: Large-scale structure of the universe — galaxies: clustering

1 Introduction

Recent observations of galaxy clustering in both photometric and spectroscopic surveys have found more relative power on large scales, $R_p \sim 20\,h^{-1}\,\mathrm{Mpc}$ ($h = H_0/100$ km/sec/Mpc), than that expected in the standard cold dark matter (CDM) model of structure formation (e.g., Maddox, etal. 1990, Efstathiou, etal. 1990, Baumgart and Fry 1991, Gramann and Einasto 1991, Hamilton, etal. 1991, Peacock and Nicholson 1991, Saunders, etal. 1991, Loveday, etal. 1992, Fisher, etal. 1992, Park, etal. 1992, Vogeley, etal. 1992, Feldman, etal. 1993). More precisely, the *shape* of the observed galaxy power spectrum $P_g(k)$ or of its Fourier transform, the two-point galaxy correlation function $\xi_g(r)$, differs on these scales from the standard CDM model prediction.

Recall that in the standard CDM model, the Universe is spatially flat, with a density $\Omega_{cdm} = 1 - \Omega_B \simeq 0.95$ in non-baryonic, weakly interacting particles which have negligible free-streaming length, and the Hubble parameter $h = 0.5$. Additionally, one posits that the density perturbations responsible for large-scale structure are adiabatic and Gaussian, with a scale-invariant primordial power spectrum $P(k) = \langle |\delta_k(t_i)|^2 \rangle \sim k$, as expected in canonical inflation scenarios. The present spectrum is related to the primordial one through the transfer function, $T(k; \Omega_i, h)$, which encodes the scale-dependence of the linear growth of perturbations, $\langle |\delta_k(t_0)|^2 \rangle = T^2(k) \langle |\delta_k(t_i)|^2 \rangle$. Finally, the galaxy power spectrum is related to the density spectrum by a bias factor b_g,

$$P_g(k) = b_g^2 T^2(k) |\delta_k(t_i)|^2 \quad . \tag{1}$$

A number of alternatives have been suggested to remedy the shape of the CDM galaxy spectrum, each of which involve modifications of one or more of the standard ingredients of the CDM model in equation (1). These include models with a lower density of cold dark matter, $\Omega_{cdm} h \simeq 0.2$, plus a cosmological constant to retain spatial flatness (Efstathiou, Sutherland, and Maddox 1990), and models with a mixture of cold and hot dark matter, $\Omega_{cdm} \simeq 0.7$, $\Omega_{hdm} \simeq 0.3$ (e.g., Schaefer, etal. 1989, van Dalen and Schaefer 1992, Taylor and Rowan-Robinson 1992, Davis, etal. 1992, Pogosyan and Starobinsky 1992, Klypin, etal. 1992). In these two cases, the transfer function $T(k)$ is flattened on scales $k^{-1} \sim R_p$ compared to standard CDM. CDM models with 'tilted' non-scale-invariant, power-law primordial spectra, $\langle |\delta_k(t_i)|^2 \rangle \sim k^n$ with $n < 1$, which arise naturally in several models of inflation, have also been recently explored (Adams, etal. 1993, Cen, etal. 1992, Gelb, etal. 1993, Liddle and Lyth 1992, Liddle, etal. 1992, Vittorio, etal. 1988). In addition, there is a growing literature on models with non-Gaussian initial fluctuations; in some cases, initial skewness and/or kurtosis can lead to enhanced structure on large scales (e.g., Moscardini, etal. 1993 and references therein). While such models can display interesting behavior of the higher order moments, in this paper we will focus on initially Gaussian fluctuations.

In all these variations on the CDM theme, one important assumption is left unchanged: that the observable galaxy distribution is related through a simple bias mechanism to the underlying matter distribution predicted by theory (e.g., Bardeen, etal. 1986). In essence, following Kaiser (1984a,b) and Bardeen (1984), one assumes that galaxies form from peaks above some global threshold in the

smoothed linear density field. In the limit of high threshold and small variance, this model is well approximated by the commonly employed linear bias scheme, in which the galaxy and mass density fields, $\delta_g(x) = (n_g(x) - \bar{n}_g)/\bar{n}_g$ and $\delta(x) = (\rho(x) - \bar{\rho})/\bar{\rho}$, are linearly related through a constant bias factor,

$$\delta_g(x) = b_g \delta(x) \quad . \tag{2}$$

This relation, implicitly assumed in equation (1), embodies the standard model for biased galaxy formation.

Early numerical evidence for biasing came from the CDM simulations of White, etal. (1987), which showed that dark matter halos are more strongly clustered than, and thus 'naturally' biased with respect to, the mass. However, since galaxy formation is a complex, non-linear process involving both gravitational and non-gravitational interactions, the relation between the mass and the galaxy distributions may be more complicated than in the peak bias model. Even purely gravitational high-resolution N-body simulations suggest that virialized halos are not always well identified with peaks in the linear density field (Katz, Quinn, and Gelb 1992).

It is therefore of interest to ask whether a more or less well-motivated modification of the standard bias scheme can generate the excess large-scale power within the context of the standard CDM model. This idea has been recently studied by Babul and White (1991) and by Bower, etal. (1993) (for precursors, see Rees 1985, Silk 1985 and Dekel and Rees 1987). The common thread in these ideas is that the bias mechanism can be modulated by environment-dependent effects. For example, in their cooperative galaxy formation scenario, Bower, etal. (1993) (hereafter BCFW) suggest that the threshold above which perturbations actually form bright galaxies may be lower in large-scale, high-density regions than elsewhere. Or perhaps baryons may be inhibited from cooling in regions photoionized by an early generation of quasars (Babul and White 1991). The net result of these feedback mechanisms is that the transformation from the density field $\delta(x)$ to the galaxy field $\delta_g(x)$ becomes *non-local* (by contrast with equation (2)), and the effective bias factor becomes scale-dependent. If the bias factor increases with scale, the galaxy spectrum will have more power at large scales, as desired. This modification of the standard CDM scenario is fundamentally different from those mentioned above: with scale-dependent bias, the extra large-scale power relative to standard CDM is only apparent, in the sense that it is only a property of the galaxy field, not the underlying mass density field; by contrast, in the other CDM variants (non-zero Λ, tilt, or mixed dark matter), there is genuine extra power in the density field.

In this paper, we consider how the higher order irreducible moments of the galaxy distribution can be used as a test of models for large-scale structure. We consider the standard CDM model and its variants with extra large-scale power (in particular, $\Omega h = 0.2$ CDM), as well as a generalized version of the non-local, scale-dependent bias scheme embodied in the cooperative galaxy formation (hereafter, CGF) model of BCFW in the context of otherwise-standard CDM. Using the results of second-order perturbation theory (Fry 1984), we compare in detail the predictions of these models for the three-point function ξ_3 with data from the Center for Astrophysics (CfA, Huchra, etal. 1983), Southern Sky (SSRS, Da Costa, etal. 1991), and Perseus-Pisces (Haynes and Giovanelli 1988) redshift surveys in the

mildly non-linear regime ($\xi_2 < 1$). Since ξ_3 is of second-order in the density perturbation amplitude for initially Gaussian fluctuations, for self-consistency we must generalize the models to include the possibility of non-linear (as well as non-local) bias and extend them from Gaussian to hierarchical matter fields. [We will use the well known result that, at least in the mildly non-linear regime, the matter field evolved gravitationally from Gaussian initial conditions leads to hierarchical statistics of the form $\langle \delta^J \rangle \propto \langle \delta^2 \rangle^{J-1}$ (cf. Fry 1984, Goroff *et al.* 1986, Bernardeau 1992).] The allowance for non-linear bias introduces an additional dimensionless parameter into the model. Even with this additional degree of freedom, we find that the CGF model tends to require rather large values of the bias parameter in order to match the 3-point function data, because scale-dependent bias modifies the correlation hierarchy, leading to a dramatic decrease of the hierarchical amplitudes Q_J at large scales, $r \gtrsim R_p$. In the context of standard CDM, such a high bias is in conflict with the COBE DMR observations of microwave anisotropy on large scales. We show that observations of the 3-point function in Fourier space, $Q(k)$, on the largest scales accessible to current redshift surveys should provide a definitive test of the CGF model and of more general models with scale-dependent bias. Our basic conclusion is that the scale-dependent bias solution to the problem of extra large-scale power affects the 3-point functions very differently from models with genuine extra power (such as CDM with $\Omega h = 0.2$). Thus, the higher-order correlations provide an important test to distinguish between different solutions of the extra power problem.

The paper is organized as follows. In section II, since it may be less familiar to the reader, we briefly review and generalize the CGF model and recapitulate the results of BCFW, demonstrating the enhancement of the two-point function on large scales required to fit the APM angular correlation function data. In section III, we review the results on the 3-point and higher order correlations in perturbation theory, focusing on the evolution of an initial Gaussian density field into a hierarchical field. In section IV, we study the higher order moments in the CGF model. Self-consistency demands that we further extend the model to include non-linear bias. In section V, we compare the standard CDM, low-density CDM, and CGF-modified CDM predictions to the data on the 3-point function from the CfA, SSRS, and Perseus-Pisces redshift surveys and we conclude in section VI.

2   Cooperative Galaxy Formation and Scale-Dependent Bias

The cooperative galaxy formation (CGF) model of BCFW is a simple phenomenological prescription for obtaining a scale-dependent bias. It starts with the standard assumptions of the CDM model, but the biasing mechanism is modified from the high peak threshold scenario. In the standard peak bias model (Kaiser 1984a, Bardeen, etal. 1986), the sites of galaxy formation are identified with peaks of the smoothed linear density field. That is, one convolves the initial density field with a filter of characteristic scale $R_g \sim 1\,h^{-1}$ Mpc, and then identifies galaxies with peaks of the smoothed field above some threshold $\nu\sigma$, i.e., with density maxima satisfying $\delta(x_{pk}) > \nu\sigma$, where $\sigma_{R_g}^2 = \langle (\rho - \bar\rho)^2 \rangle / \bar\rho^2$ is the variance of the smoothed field, and ν sets the threshold height. (Hereafter, we implicitly assume the field $\delta(x)$ is smoothed on the scale R_g.) For example, for an infinitely sharp threshold, the galaxy field is $\delta_g(x_{pk}) = \theta(\delta(x_{pk}) - \nu\sigma)$. The combination of the threshold peak height ν and the spatial smoothing

scale R_g is chosen so that the density of peaks reproduces the observed abundance of luminous galaxies; moreover, these parameters are taken to be global, spatially invariant quantities. In the limit of high threshold ($\nu \gg 1$) and small variance, the two-point correlation function of the peaks is enhanced over that of the mass by an approximately constant factor (Kaiser 1984a),

$$\xi_{pk}(r; \nu) \simeq \left(\frac{\nu^2}{\sigma^2}\right) \xi(r) \quad , \tag{3}$$

where $\xi(r) = \langle \delta(x)\delta(x+r) \rangle$. Since $\xi(r)$ is quadratic in the density field, this is equivalent to the linear bias model of equation (2), with the identification of the bias factor as $b_g = (\nu/\sigma)$. Following Kaiser (1984a) and BCFW, we will apply this model to regions above the threshold, $\delta(x) > \nu\sigma$, rather than to maxima; this simplifies the model while retaining its important features.

BCFW extend the standard bias model by replacing the universal threshold ν with a threshold that depends on the mean mass density in a surrounding 'domain of influence' of characteristic size $R_s > R_g$. The motivation is to model the possibility that peaks form galaxies more easily (or perhaps form brighter galaxies which are included in a magnitude-limited catalog) if there are other peaks nearby–thus the name cooperative galaxy formation. Specifically, they assume that galaxies form from regions satisfying

$$\delta(x) > \nu\sigma - \kappa\bar{\delta}(x; R_s) \quad , \tag{4}$$

where $\bar{\delta}(x; R_s)$ is the density field smoothed on the scale R_s, and κ is the modulation coefficient of the threshold. If $\kappa > 0$, the threshold for galaxy formation is lower in "protosupercluster" regions than in "protovoids". The parameters R_s and κ parametrize the scale and strength of cooperative effects; they are also constrained by the observed galaxy abundance.

The model of equation (4) is equivalent to applying the standard threshold bias model to the new density field defined by

$$\delta'(x) \equiv \delta(x) + \kappa\bar{\delta}(x; R_s) \quad , \tag{5}$$

that is, to imposing the condition $\delta' > \nu\sigma$. Note that δ' is a Gaussian random field if the underlying density field δ is Gaussian. Here we consider a generalization of the CGF model: instead of applying a sharp threshold clipping to $\delta'(x)$, we assume that the galaxy field is an arbitrary continuous function of the field δ',

$$\delta_g(x) = f(\delta'(x)) = f\left[\delta(x) + \kappa\bar{\delta}(x; R_s)\right] \quad . \tag{6}$$

For example, in the limit of high threshold, for the standard bias model the function f is approximately an exponential, $f(x) = \exp(\nu x/\sigma)$ (Kaiser 1984b, Politzer and Wise 1984). We assume that f is expandable in a Taylor series in its argument,

$$\delta_g = f(\delta') = \sum_{k=1}^{\infty} \frac{b_k}{k!} \delta'^k \quad . \tag{7}$$

BCFW compute the two-point correlation function for the CGF model on large scales, using the CDM density spectrum derived from linear perturbation theory. In this regime, our generalized CGF model

reduces to the linear bias model applied to the field δ',

$$\delta_g(x) = b_g \delta'(x) = b_g \left[\delta(x) + \kappa \bar{\delta}(x; R_s) \right] \tag{8}$$

where we have identified $b_g = b_1$. That is, by working only to linear order in perturbation theory, one should self-consistently include only the first (linear) term in the series of equation (7). Conversely, when we consider second order perturbations below, we can and should include the possibility of quadratic ($k = 2$) bias.

Comparing equation (8) with equation (2), it is clear that cooperative effects boost the galaxy power spectrum on large scales relative to the standard global bias model. Taking a Gaussian filter for the smoothed density field,

$$\bar{\delta}(x; R_s) = \left(2\pi R_s^2\right)^{-3/2} \int d^3r \delta(r) \exp\left(-\frac{|x - r|^2}{2R_s^2}\right) \quad , \tag{9}$$

the Fourier transforms of the density fields satisfy

$$\delta'(k) = \delta(k) \ [1 + \kappa \mathcal{G}(k)] \quad , \tag{10}$$

where $\mathcal{G}$ is the Fourier transform of the window filter in $\bar{\delta}(x; R_s)$,

$$\mathcal{G}(k) = \mathcal{G}(k) = e^{-(kR_s)^2/2} \quad , \tag{11}$$

with $k = |k|$. The galaxy power spectrum, $P_g(k) = \langle |\delta_g(k)|^2 \rangle$, is thus related to the density power spectrum, $P(k) = \langle |\delta(k)|^2 \rangle$, by

$$P_g(k) = b_g^2 P'(k) = b_g^2 \left[1 + \kappa \mathcal{G}(k)\right]^2 P(k) \equiv b_{\text{eff}}^2(k) \ P(k) \quad . \tag{12}$$

This expression makes manifest how cooperative effects result in an effective scale-dependent bias, $b_{\text{eff}}(k) = b_g[1 + \kappa \mathcal{G}(k)]$. On small lengthscales, $k^{-1} \ll R_s$, equation (12) implies the usual bias factor, $b_{\text{eff}}(k \to \infty) \simeq b_g$, while on large scales, $k^{-1} \gg R_s$, the effective bias factor is increased to $b_{\text{eff}}(k \to 0) \simeq b_g(1 + \kappa)$. In the parameter range studied by BCFW, the choice $\kappa = 2.29$, $R_s = 20 \, h^{-1}$ Mpc appears to give the best fit to the observed extra large-scale power for CDM when compared to the APM angular correlation function, and we shall focus mainly on this case. We see that this choice boosts the galaxy power spectrum on scales $k \lesssim 0.05h$ Mpc^{-1} by over a factor of ten.

To see what these effects look like graphically for the CDM model, we consider the linear CDM density power spectrum of Davis, etal. (1985),

$$P(k) = A\sigma_8^2 k \left(1 + \frac{1.7k}{\Omega h} + \frac{9k^{3/2}}{(\Omega h)^{3/2}} + \frac{k^2}{(\Omega h)^2}\right)^{-2} \quad , \tag{13}$$

where the wavenumber k is in units of h Mpc^{-1}. Here the normalization is set as usual in terms of the variance of the linear mass fluctuation within spheres of radius $8 \, h^{-1}$ Mpc, $\sigma_8 \equiv \langle (\delta M/M)^2 \rangle_{R=8h^{-1}\text{Mpc}}^{1/2}$, where

$$\sigma_R^2 = \frac{1}{2\pi^2} \int\limits_0^\infty dk k^2 P(k) W^2(kR) \quad , \tag{14}$$

and the top-hat window function

$$W(kR) = \frac{3}{(kR)^3}(\sin kR - kR \cos kR) \tag{15}$$

filters out the contribution from small scales. For standard CDM with $\Omega h = 0.5$, this gives $A = 2.76 \times 10^5 (h^{-1}\,\mathrm{Mpc})^3$.

Substituting the CDM power spectrum with $\Omega h = 0.5$ into equation (12), we find the galaxy two-point correlation function for the CGF model

$$\xi_g(r) = \frac{1}{2\pi^2} \int dk\ k^2 \frac{\sin kr}{kr} P_g(k)\ , \tag{16}$$

shown in Fig. 1 (the curve labelled CGF, with $\kappa = 2.29$, $R_s = 20\,h^{-1}\,\mathrm{Mpc}$). Note that we actually plot $\xi_g(r)/(b_g\sigma_8)^2$, where b_g is the constant factor in equation (8). Redshift surveys of optically selected galaxies (in particular the CfA and Stromlo-APM surveys) indicate that the variance in galaxy counts on 8 $h^{-1}\,\mathrm{Mpc}$ scale is of order unity. Thus, in a linear, scale-independent bias model, the bias factor for these galaxies would be expected to be $b_{opt} \simeq 1/\sigma_8$; for other galaxy populations, however, $b_{gal}\sigma_8$ may differ from unity. For comparison, in Fig. 1 we also show the two-point function for standard CDM ($\Omega h = 0.5$, $\kappa = 0$) and for a low-matter-density CDM model ($\Omega h = 0.2$). Both the CGF model and the low-density CDM model have sufficient relative large-scale power to approximately reproduce the observed galaxy angular correlation function $w(\theta)$ inferred from the APM survey (BCFW, Maddox, etal. 1990, Efstathiou, Sutherland, and Maddox 1990). This level of extra power is also broadly consistent with that inferred from the power spectrum of IRAS galaxies (Feldman, etal. 1993, Fisher, etal. 1992) and the redshift-space two-point function $\xi(s)$ inferred from the Stromlo-APM survey (Loveday, etal. 1992). The CGF curve in Fig. 1 should be compared to that in Fig. 2 of BCFW. Note that the linear bias approximation used here (equation (8)) differs from the non-linear threshold formula of BCFW (Cf. their eqn.(10)), but that our final result for $\xi(r)$ is very similar to theirs.

Thus, cooperative effects can mimic extra large-scale power in the galaxy two-point function, while the other remedies for CDM, such as low-density, mixed dark matter, or tilted ($n < 1$) models, have genuine extra large-scale power in the spectrum. How can we discriminate between these choices for extra large-scale power, that is, between real power and the illusion of power? Below, we argue that the three-point function can provide a distinguishing test, at least for models with Gaussian initial fluctuations. The reason is that the galaxy three-point function induced by gravitational evolution depends in large measure on the two-point function of the *mass*.

Before turning to higher order correlations, we remark that the treatment given here and below applies more generally than to the CGF model, and in fact to any model with scale-dependent bias. That is, the chain of reasoning above is invertible: if the galaxy and density power spectra are related by a scale-dependent bias, $P_g(k) = b^2(k)P(k)$, we can always think of the galaxy field $\delta_g(x)$ as arising from some non-local transformation of the density field $\delta(x)$. To see this, let $b^2(k) = b_g^2 f^2(k)$, where b_g is a constant and we assume that $f^2(k)$ has a limit, $f^2(k \to \infty) = 1$. Then consider the field $\delta'(k) = \delta_g(k)/b_g = f(k)\delta(k)$. We can write $f(k) = 1 + \kappa G(k)$, where $\lim G(k \to \infty) = 0$, and we can

choose κ such that $\lim G(k \rightarrow 0) = 1$, so that $\delta'(k) = \delta(k)[1 + \kappa G(k)]$. Comparing with equation (10), we see that this expression, where $G(k)$ is interpreted as the Fourier transform of some window function (which in general will not be a Gaussian), is all that we need for the results discussed here and below to go through. Provided the function $b(k)$ is not too pathological, this Fourier transform should exist.

3 3-point correlation function in perturbation theory

We want to consider how scale-dependent bias, as embodied for example in the CGF model, affects the higher order correlation functions. The motivation for this study is that the galaxy three-point function is observed to scale in a particular way with the two-point function, and both perturbation theory and N-body simulations show that this scaling can arise via non-linear gravitational evolution from Gaussian initial fluctuations. Since scale-dependent bias introduces a different scale behavior into the problem, we would expect it to be manifest as a change in the scaling behavior of the higher order correlations. We will work in the context of second-order perturbation theory (Fry 1984), the results of which we review here before discussing how they are modified by scale-dependent bias. The perturbative approach should be valid in the mildly non-linear regime, $\delta \lesssim 1$. In the range where they overlap, the second-order perturbation theory results below for S_3 in standard CDM appear to be quite consistent with the N-body simulations of Bouchet and Hernquist (1992).

Defining the Fourier transform of the density field,

$$\delta(k) = \frac{1}{V} \int d^3 x \delta(x) e^{i\mathbf{k} \cdot \mathbf{x}} \quad , \tag{17}$$

we consider the two- and three-point correlation functions in k-space, $\langle \delta(k_1)\delta(k_2) \rangle$ and $\langle \delta(k_1)\delta(k_2)\delta(k_3) \rangle$, which are the Fourier transforms of the spatial two- and three-point functions $\xi_2(x_1, x_2)$ and $\xi_3(x_1, x_2, x_3)$. By homogeneity and isotropy, the k-space moments are non-zero only for $\sum k_i = 0$,

$$\langle \delta(k_1)\delta(k_2) \rangle = \delta_{\mathbf{k_1} + \mathbf{k_2}, 0} P(k_1) \quad , \quad \langle \delta(k_1)\delta(k_2)\delta(k_3) \rangle = \delta_{\mathbf{k_1} + \mathbf{k_2} + \mathbf{k_3}, 0} B(k_1, k_2, k_3) \quad . \tag{18}$$

This defines the power spectrum $P(k) = \langle |\delta(k)|^2 \rangle$ and the bispectrum $B_{123} = B(k_1, k_2, k_3)$.

Early observations of clustering on small scales (Groth and Peebles 1977) suggested that the galaxy two- and three-point functions obey a scaling hierarchy,

$$\xi_3(x_1, x_2, x_3) = Q \left[\xi_2(x_1, x_2)\xi_2(x_2, x_3) + (1 \leftrightarrow 2) + (2 \leftrightarrow 3) \right] \tag{19}$$

with $Q = \text{constant} \sim 1$, roughly independent of the size and shape of the triangle formed by the points x_1, x_2, x_3. If the scaling of equation (19) holds exactly, then the hierarchical 3-point amplitude Q is also related to the bispectrum by the k-space version of equation (19) (Fry and Seldner 1982),

$$Q \equiv \frac{B_{123}}{P_1 P_2 + P_1 P_3 + P_2 P_3} \quad , \tag{20}$$

with $P_i \equiv P(k_i)$. We will consider equation (20) as the definition of the amplitude Q, even if it is not constant. In the strongly non-linear regime $\delta \gg 1$, N-body simulations of CDM and power-law spectrum

models do seem to display the approximate shape- and size-indepedence of equation (19) (Fry, Melott, and Shandarin 1993). However, in second-order perturbation theory in the mildly non-linear regime, while Q as defined in equation (20) obeys the scaling with size, it does depend on the shape of the configuration in k-space.

To calculate the three-point function in the weakly non-linear regime, one expands the perturbation equations in powers of δ, $\delta(x,t) = \delta^{(1)}(x,t) + \delta^{(2)}(x,t) + ...$, where $\delta^{(1)}$ is the linear solution, and $\delta^{(2)} = \mathcal{O}(\delta^{(1)})^2$ is the second-order solution, obtained by using the linear solution in the source terms. For Gaussian initial fluctuations, the three-point function vanishes to linear order, $\langle \delta^{(1)}(x_1)\delta^{(1)}(x_2)\delta^{(1)}(x_3) \rangle = 0$, and the lowest order contribution to the bispectrum is $B_{123} = \langle \delta^{(1)}(k_1)\delta^{(1)}(k_2)\delta^{(2)}(k_3) \rangle + (1 \leftrightarrow 3) + (2 \leftrightarrow 3)$, with the result

$$B_{123} = \left[\frac{10}{7} + \left(\frac{k_1 \cdot k_2}{k_1 k_2} \right) \left(\frac{k_1}{k_2} + \frac{k_2}{k_1} \right) + \frac{4}{7} \left(\frac{k_1 \cdot k_2}{k_1 k_2} \right)^2 \right] P_1 P_2 + (1 \leftrightarrow 3) + (2 \leftrightarrow 3) \qquad (21)$$

(Fry 1984). Strictly speaking, this result holds for initially Gaussian fluctuations in a matter-dominated universe with $\Omega = 1$, but the work of Juszkiewicz and Bouchet (1991) shows that the dependence of the three-point function on Ω is extremely slight. A particular case of importance is that of equilateral triangle configurations in k-space, $k_1 = k_2 = k_3$, for which $Q(k) \equiv Q_\Delta = 4/7$, independent of $P(k)$. The independence of this result of the power spectrum makes it a useful quantity for distinguishing gravitational from non-gravitational (e.g., bias) effects. (In general, for other configurations or averages over configurations, there will be a small dependence on $P(k)$.) In section IV, we will see how this result is modified by constant and scale-dependent bias, and compare these predictions with observations.

Another useful and increasingly popular characterization of the three-point amplitude, which does depend on $P(k)$, is the hierarchical averaged amplitude S_3,

$$S_3(V) = \frac{\bar{\xi}_3(V)}{\bar{\xi}_2^2(V)} = \frac{\langle \delta^3(x; V) \rangle}{\langle \delta^2(x; V) \rangle^2} \quad . \qquad (22)$$

Here $\bar{\xi}_2$ and $\bar{\xi}_3$ are the 2-point and 3-point density correlation functions averaged over a window function $W(r)$ of characteristic volume V:

$$\begin{aligned} \bar{\xi}_2(V) &= \frac{1}{V^2} \int \int d^3r_1 d^3r_2 \, \xi_2(|r_1 - r_2|) W(r_1) W(r_2) \\ \bar{\xi}_3(V) &= \frac{1}{V^3} \int \int \int d^3r_1 d^3r_2 d^3r_3 \, \xi_3(r_1, r_2, r_3) W(r_1) W(r_2) W(r_3) \end{aligned} \qquad (23)$$

In comparing with model predictions, it is useful to think of S_3 as the ratio of moments of the density field $\delta(x; V)$ smoothed over the volume V (Cf. equation (22)),

$$\delta(x; V) = \frac{1}{V} \int d^3r \, \delta(x + r) W(r) \quad . \qquad (24)$$

Thus, $\bar{\xi}_2(V)$ is just the variance of the smoothed density field, given by equation (14), and $\bar{\xi}_3(V)$ is its skewness. (The smoothing discussed here should not be confused with the smoothed density field introduced in the CGF model of equation (5); in the CGF model, the smoothing radius is associated

with the physical scale of threshold modulation effects, while here it merely defines the resolution with which one observationally probes the density field.)

Following standard practice, we evaluate S_3 with a top-hat window: for the volume $V = 4\pi R^3/3$, $W(r) = 1$ for $r < R$ and vanishes for $r > R$; its Fourier transform $W(kR)$ is given by equation (15). In this case, $\bar{\xi}_2$ and $\bar{\xi}_3$ are related to the moments of counts in cells of volume V, and the skewness is given by

$$\langle \delta^3(R) \rangle = \frac{3}{(2\pi)^6} \int \int d^3k_1 d^3k_2 B(k_1, k_2, |\mathbf{k}_1 + \mathbf{k}_2|) W(k_1 R) W(k_2 R) W(|\mathbf{k}_1 + \mathbf{k}_2|R) . \qquad (25)$$

In Fig.2, we plot S_3 as a function of the top-hat smoothing radius R for CDM power spectra with $\Omega h = 0.5$ and $\Omega h = 0.2$ (Cf. (13)), using the second-order perturbation theory result (21) for the bispectrum (and assuming that the smoothing radius R is much larger than the galaxy smoothing radius $R_g \sim 1\, h^{-1}\, \mathrm{Mpc}$). In computing S_3 for the low-density model, we have ignored the tiny correction for $\Omega \neq 1$ (Juszkiewicz and Bouchet 1991). The result for the CGF model, also shown here, will be discussed below in section IV. So far as we are aware, these numerical results for S_3 for CDM are new. (Goroff et al. 1986 roughly integrated S_3 for CDM with a Gaussian smoothing window using Monte Carlo integration, and we have also studied S_3 for Gaussian smoothing. Top hat smoothing requires a more accurate numerical integrator, and we have checked our integration code by comparing with the analytic results of Juszkiewicz and Bouchet (1991) for S_3 for power law spectra–see below). Where our results overlap with the N-body results of Bouchet and Hernquist (1992), the agreement is quite good. We see that S_3 does vary with scale R in a manner that depends on the shape of the power spectrum, because the CDM spectrum is not exactly scale-free. For a scale-free, power-law spectrum $P(k) \propto k^n$, R can be scaled out of the expression for S_3, i.e., S_3 is a constant, and its value can be found analytically, $S_3(R) = 34/7 - (n + 3)$ (Juszkiewicz and Bouchet 1991). On the other hand, for a purely unsmoothed field, $R = 0$, $W(kR) = 1$, the normalized skewness is $S_3(0) = 34/7$, independent of the power spectrum (Peebles 1980).

The hierarchical behavior of the three-point function in perturbation theory extends to higher order correlations, so one can define higher order hierachical amplitudes $Q_J \simeq \xi_J/\xi_2^{J-1}$ or $S_J = \bar{\xi}_J/\bar{\xi}_2^{J-1}$ which have characteristic amplitudes set by gravitational instability (see Peebles 1980, Fry 1984, Goroff et al. 1986, Bernardeau 1992).

4 Scale-dependent bias and the 3-point correlations

We now turn to study how the J-point correlation amplitudes, and in particular the three-point function, are affected by constant and scale-dependent biasing. Because we consider the 3-point function ξ_3, we must extend the CGF model to the case in which the matter distribution is not just Gaussian but hierarchical, i.e., we consider the contribution of second-order gravitational evolution. Fry and Gaztañaga (1993a) have shown that the first-order contribution of biasing to ξ_3 is comparable to the contribution from second-order gravitational evolution and, thus, it is not consistent to assume a purely Gaussian density field. We first consider how the non-local cooperative modulation of the density field

affects the 3-point function, and then study how it is further affected by linear and non-linear bias, that is, we consider the sequence of transformations $\delta \rightarrow \delta' \rightarrow \delta_g$.

4.1 Cooperative bias

Consider the effect on the 3-point amplitude of the non-local, cooperative linear transformation of the density field given in equation (10). The bispectrum of the cooperative field $\delta'(x)$ is

$$B'_{123} = B_{123} (1 + \kappa\mathcal{G}_1)(1 + \kappa\mathcal{G}_2)(1 + \kappa\mathcal{G}_3) \quad , \tag{26}$$

where $\mathcal{G}_i \equiv \mathcal{G}(k_i)$ is given by equation (11). The hierarchical 3-point amplitude Q' of the field δ', defined in equation (20), can be expressed in terms of the 3-point amplitude Q for the underlying density field, δ:

$$Q' = Q \frac{(P_1 P_2 + P_1 P_3 + P_2 P_3)(1 + \kappa\mathcal{G}_1)(1 + \kappa\mathcal{G}_2)(1 + \kappa\mathcal{G}_3)}{P_1 P_2 (1 + \kappa\mathcal{G}_1)^2 (1 + \kappa\mathcal{G}_2)^2 + (1 \leftrightarrow 3) + (2 \leftrightarrow 3)} \quad . \tag{27}$$

Note that the ratio Q'/Q has no explicit angular dependence in k-space, i.e., it depends only on the magnitudes k_1, k_2, k_3. Using this property, we can point to several important limiting behaviors of Q'/Q. For example, on small length scales, $k_1, k_2, k_3 \gg R_s^{-1}$, we obviously retrieve $Q' = Q$, and in the opposite limit of large scales (small triangles in k-space), $k_1, k_2, k_3 \ll R_s^{-1}$, we have $Q'/Q \simeq 1/(1 + \kappa)$, independent of the power spectrum and the triangle configuration. The other limiting case of interest is a triangle with two large sides and one small side, e.g., $k_1, k_2 \gg R_s^{-1}$, $k_3 \ll R_s^{-1}$: if the power spectrum is approximately a power law, $P(k) \propto k^n$, then for $n > 0$ (and $k_3/k_{1(2)} \ll (1 + \kappa)^{-2/n}$), $Q'/Q \simeq 1 + \kappa$; for $n = 0$, $Q'/Q = 3(1 + \kappa)/[1 + 2(1 + \kappa)^2]$; and for $n < 0$, $Q'/Q \simeq 1/(1 + \kappa)$.

As noted in section III, an important class of configurations is equilateral triangles in k-space, $k_1 = k_2 = k_3 = k$, for which

$$Q'_\Delta = Q_\Delta \frac{(1 + \kappa\mathcal{G})^3}{(1 + \kappa\mathcal{G})^4} = \frac{Q_\Delta}{(1 + \kappa\mathcal{G})} \quad . \tag{28}$$

With the Gaussian CGF smoothing window, $\mathcal{G}(k) = e^{-(kR_s)^2/2}$, for scales larger than R_s, $kR_s \ll 1$, we have $Q'_\Delta = Q_\Delta (1 + \kappa)^{-1}$, whereas for scales smaller than R_s, $kR_s \gg 1$, we have $Q'_\Delta = Q_\Delta = 4/7$. For the preferred parameter values considered by BCFW to match the APM data, $R_s = 20 \, h^{-1}$ Mpc and $\kappa = 2.29$, we see that within the range of the weakly non-linear regime, $k^{-1} \sim 10 \, h^{-1}$ Mpc, there is a sharp transition from $Q'_\Delta \simeq Q_\Delta$ to $Q'_\Delta = 0.3 Q_\Delta$. We explore the observational consequences of this behavior in the next section (see Fig. 3).

It is also of interest to study the normalized skewness of the smoothed cooperative density field, $S'_3(R) = \langle \delta'^3(x; R) \rangle / \langle \delta'^2(x; R) \rangle^2$, where the Fourier-transform of the top-hat-smoothed cooperative density field is $\delta'(k; R) = W(kR)\delta(k)[1 + \kappa\mathcal{G}(kR_s)]$, with $W(kR)$ given by (15) and $\mathcal{G}(kR_s)$ given by (11). The function $S'_3(R)$ is shown, for the CDM $\Omega h = 0.5$ spectrum with the canonical CGF parameters $\kappa = 2.29$, $R_s = 20 \, h^{-1}$ Mpc, as the curve labelled CGF in Fig. 2. As expected, in this case S_3 has a steeper dependence on R for scales $R \lesssim R_s$ than either the standard or low-density CDM models, due to the rather sharp, non-power-law feature in $\delta'(k)$ arising from cooperative effects. These different behaviors are compared with data in Fig. 4 below.

One can also define higher order amplitues, Q_J, by $\langle \delta^J(k) \rangle \simeq Q_J P^{J-1}$, with $Q_3 = Q$. From the above arguments it is straightforward to show that, in general, for regular J-sided polygons in k-space,

$$Q'_J = \frac{Q_J}{(1 + \kappa \mathcal{G})^{J-2}} \tag{29}$$

Again, for a Gaussian filter $\mathcal{G}$, we have $Q'_J = Q_J (1 + \kappa)^{-J+2}$ for $kR_s \ll 1$ and $Q'_J = Q_J$ for $kR_s \gg 1$. Thus if the underlying density field $\delta(x)$ is hierarchical, with Q_J approximately constant as a function of k, the new field δ' is also hierarchical, $\langle \delta'^J \rangle = Q'_J \langle \delta'^2 \rangle^{J-1}$, with the hierarchical amplitudes Q'_J varying with scale from $Q'_J = Q_J$ to $Q'_J = Q_J (1 + \kappa)^{-J+2}$.

4.2 Non-linear, local bias

In the previous subsection, we considered the three-point function for the cooperative density field $\delta'(x)$ defined in equation (5). We now want to relate this to the three-point function of the galaxy field $\delta_g(x)$, defined by the arbitrary, local, non-linear transformation of the cooperative field in equation (6). Fry & Gaztañaga (1993a) have shown that, in the weakly non-linear limit $\langle \delta^2 \rangle < 1$, the hierarchical relation between the moments of the density field, $\langle \delta^j \rangle \propto \langle \delta^2 \rangle^{j-1}$, is preserved under an arbitrary local transformation of this form. Nevertheless, the higher order moments of the galaxy field will differ quantitatively from the hierarchical amplitudes of the cooperative field. The analysis of Fry & Gaztañaga (1993a) is valid as long as the amplitudes of the original field (here, the cooperative field $\delta'(x)$) are of zeroth order in the two-point function $\xi_2 = \langle \delta'^2 \rangle$, i.e., under the assumption that $Q'_J = \mathcal{O} \langle \delta'^2 \rangle^0$; in particular, their results apply even if the original field is not hierarchical in the strict sense that Q'_J is constant.

Let the hierarchical amplitudes of the smoothed galaxy field $\delta_g(x) = f(\delta')$ be denoted by $Q_{g,J}$. To consider the 3-point galaxy amplitude, $Q_g \equiv Q_{g,3}$, we must keep terms up to quadratic order in δ' in the expansion (7) of the biasing function $f(\delta')$. Applying the results of Fry and Gaztañaga (1993a), we find

$$Q_g = b^{-1}(Q' + c_2) + \mathcal{O} \langle \delta'^2 \rangle \quad , \tag{30}$$

where $c_2 = b_2/b$ and $b = b_1$ in equation (7), and Q', the 3-point amplitude for the cooperative field δ', is related to the 3-point amplitude of the underlying density field by equation (27). For example, for the high peaks model, in the limit $\nu \gg 1$ and $\sigma \ll 1$, the bias function $f(\delta')$ is exponential, and we have $c_2 = b$. This suggests that the c_2 term in (30) is of the same order as the Q' term, i.e., that the contribution of non-linear bias to the galaxy 3-point function may be comparable to the second-order gravitational contribution. For equilateral triangles in k-space, we can use (28) and (30) to relate the galaxy 3-point amplitude $Q_{g,\Delta}$ to that of the underlying density field, Q_Δ,

$$Q_{g,\Delta} = b^{-1} \left(\frac{Q_\Delta}{1 + \kappa \mathcal{G}} + c_2 \right) \quad , \tag{31}$$

with $Q_\Delta = 4/7$. On small scales, $k_{NL} \gg k \gg R_s^{-1}$, where cooperative effects are negligible, but still in the mildly non-linear regime $\langle \delta^2 \rangle < 1$, we have $Q_{g,SS} \simeq b^{-1}(Q + c_2)$, just the result in the

absence of cooperative effects. On large scales, $k \ll R_s^{-1}$, the galaxy 3-point amplitude is $Q_{g,LS} \simeq b^{-1}[(1+\kappa)^{-1}Q + c_2]$. The fractional change in Q_g between large ($kR_s < 1$) and small ($kR_s > 1$) scales is thus

$$\frac{\Delta Q_g}{Q_g} \simeq \left(\frac{\kappa}{1+\kappa}\right) \frac{Q}{bQ_g} \quad . \tag{32}$$

For the case of purely linear biasing, $c_2 = 0$, this gives $\Delta Q_g/Q_{g,SS} \simeq \kappa/(1+\kappa)$, independent of b or Q.

A similar expression can be derived for the hierarchical amplitudes $S_J = \bar{\xi}_J/\bar{\xi}_2^{J-1}$ of the volume-averaged correlation functions. Following the arguments above, the small-to-large-scale variation in the galaxy 3-point amplitude $S_g \equiv S_{g,3}$ is related to the density amplitude $S \equiv S_3$ by

$$\frac{\Delta S_g}{S_g} \simeq \left(\frac{\kappa}{1+\kappa}\right) \frac{S}{bS_g} \quad . \tag{33}$$

Again for purely linear bias, this gives $\Delta S_g/S_{g,SS} \simeq \kappa/(1+\kappa)$.

Finally, for the non-CGF models, note that equation (30) relates the galaxy and matter density 3-point amplitudes with the replacement $Q' \to Q$ (Fry and Gaztañaga 1993a); we will make use of this in comparing the CDM models to observations below. It is also worth reiterating that all of our results apply to models with initially Gaussian fluctuations. For non-Gaussian models, there is an additional first-order contribution to the 3-point amplitude, which can be thought of as a (possibly scale-dependent) contribution to the parameter c_2.

5 Comparison with observations

We now compare the model predictions for the three-point amplitudes with observations from the CfA, SSRS, and Perseus-Pisces redshift surveys. As above, we focus on three models: standard CDM ($\Omega h = 0.5$), low-density CDM ($\Omega h = 0.2$), and CGF-modified standard CDM, and we employ the results of second-order perturbation theory. Comparison with the observed galaxy amplitudes, $S_{g,3}$ and $Q_{g,\Delta}$, can in principle be used to constrain the bias parameters b and c_2 as well as the CGF parameters κ and R_s. In combination with other observations, e.g., of the galaxy power spectrum, and of the large-angle microwave anisotropy as seen by COBE DMR and other experiments, these results can help point toward preferred models for large-scale structure.

5.1 Limits from Q_Δ

Baumgart and Fry (1991) have estimated the galaxy power spectrum and the Fourier-space three-point amplitude for equilateral triangle configurations, Q_Δ, using data from the Center for Astrophysics and Perseus-Pisces redshift surveys. It is worth noting that the power spectrum $P(k)$ for these samples does show evidence for the extra large-scale power inferred in other spectroscopic (e.g., IRAS) and photometric (e.g., APM) surveys. Their results for $Q_\Delta(k)$, averaged over 3 subsamples each from the CfA and Perseus-Pisces surveys, are shown in Fig. 3. The errors bars in each bin indicate the variance between subsamples, and we only show results for values of the wavenumber away from the strongly non-linear regime.

The striking feature of these results is the relative constancy of the three-point amplitude over more than a decade in wavenumber, $k = 0.1 - 1.6 (h^{-1} \text{Mpc})^{-1}$. Moreover, the observed amplitude of Q_Δ over this range is apparently in reasonable agreement with the prediction of second-order perturbation theory *without* cooperative effects, and under the assumption of no bias, $b = 1$, $c_2 = 0$, namely $Q_\Delta = 4/7$ (shown as the short-dash line in Fig. 3). Turning this around, using the perturbation theory relation $Q_{g,\Delta} = b^{-1}[(4/7) + c_2]$, one can in principle use the results in Fig. 3 to constrain the parameter space of $b - c_2$ for any model with scale-independent bias. In practice, however, the derived constraints are not terribly stringent. First, searching this two-dimensional space and treating the data points as independent, one finds a minimum $\chi^2 \simeq 25.5$ (for 12 data points and a 2-parameter fit, i.e., 10 degrees of freedom) for $c_2 \simeq 0.52 b - (4/7)$. This is consistent with a mean value of $Q_\Delta \simeq 0.52$ over the plotted range of k, close to the expected perturbation theory result of $4/7 = 0.57$. In particular, for purely linear bias, $c_2 = 0$, the best fit value of the bias parameter is $b = 1.1 \pm 0.1$, consistent with the visual impression from Fig. 3. On the other hand, this constraint on the bias parameter space should be interpreted with a great deal of caution, since the best fit curve for perturbation theory has a chi-squared of 2.5 per degree of freedom, more than 3-σ above the expected value. A better fit to the data would be obtained with a model in which Q_Δ falls gently with increasing k. However, given the likelihood that the true data errors are larger than those shown here, it would certainly be premature to exclude the perturbation theory result on this basis.

The statements above apply for local, non-cooperative bias models. On the other hand, as noted in section 4.1, the CGF model predicts a dramatic scale-dependence of $Q_\Delta(k)$ around the scale $kR_s \sim 1$. This behavior is shown in Fig. 3 for the 3 CGF parameter choices considered by BCFW, $\kappa, R_s = 0.84, 10 \, h^{-1} \, \text{Mpc}$ (dot-long dash curve), 2.29, $20 \, h^{-1} \, \text{Mpc}$ (solid curve), and 4.48, $30 \, h^{-1} \, \text{Mpc}$ (dot-short dash curve). As above, these models are plotted for $c_2 = 0$, $b = 1$. The 'smoking gun' of these models is the sharp downturn in Q_Δ on large scales. Since, within the observational errors, no such downturn is observed, one can use this to constrain the CGF parameter space. In particular, for $R_s = 10 \, h^{-1} \, \text{Mpc}$, $\kappa = 0.84$, the CGF model is always a significantly poorer fit to the data than the scale-independent bias models. For this choice of CGF parameters, the requirement of a fit that is within 1-σ of the scale-independent models (i.e., a fit with $\chi^2 < 3$ per degree of freedom) necessitates a linear bias parameter $b > 2.6$ and a significant non-linear bias, $c_2 > 0.8$. In this case, the large linear bias factor suppresses the gravitational and cooperative contribution to Q, and the match with the observations is obtained chiefly by the non-linear bias. This would make the apparent agreement between the observed Q_Δ and the perturbation theory prediction of 4/7 purely coincidental. This behavior is an instance of our general conclusion that models with sharply varying scale-dependent bias are forced to uncomfortably large values of the linear bias b. On the other hand, for larger values of the CGF 'scale of influence' R_s, the 3-point data do not extend to large enough scales for the downturn to be significant. Consequently, the $R_s = 20 \, h^{-1} \, \text{Mpc}$ CGF model, when fitted to the $Q_\Delta(k)$ data, occupies the same region in the two-dimensional $b - c_2$ bias parameter space, with only a slightly higher χ^2 than the non-CGF models. Clearly, to more strongly constrain or rule out the CGF model, it would be useful to have data on

$Q_\Delta(k)$ which extends down to $k \lesssim 0.05$ h Mpc^{-1}; this should be feasible with currently available redshift samples drawn from the IRAS catalog.

5.2 Limits on S_3

To compare model predictions to observations of the volume-averaged normalized skewness S_3, we use the results of the S_3 analysis by Gaztañaga (1992) for samples in the CfA and SSRS redshift catalogs (we use the largest samples, denoted SSRS115 and CfA92 in Gatañaga 1992). The average over these samples is shown in Fig. 4, where we plot $S_{g,3}$ as a function of top-hat smoothing radius (or cell size) R. Each data point in Fig. 4 is an average over bins that correspond to different degrees of freedom: for a given value of R, the average number of galaxies in that cell size is at least one unit larger than in the cell of the next smallest value of R shown in the figure. The errorbars shown here are the larger of the intersample dispersion in the given R-bin and the intrinsic errors in the original samples. From Fig. 4, it is apparent that $S_{g,3}(R) \simeq 2$ is quite constant over the range of R shown, with a variation of about 25%. We also show in Fig. 4 the same model predictions for S_3 as in Fig. 2, again for the bias parameters $b = 1$ and $c_2 = 0$. The reader should mentally note that the curves in Fig. 4 can be shifted vertically, and have their slopes magnified or depressed, by changing the values of b and c_2.

In Fig. 5 we plot the contours of χ^2 for the comparison between the three models and the S_3 observations in the $b - c_2$ parameter space. The 3 contours correspond to $\chi^2 = 5$, 8, and 14 for 11 data points fit with 2 parameters (9 degrees of freedom). Again, because of the way error bars have been assigned to the data, we caution against absolute interpretations of these χ^2 values; however, the difference in χ^2 values for different models should provide a measure of the relative goodness of fit to the data. In this sense, both CDM models give comparably good fits to the data for values of the bias parameter above $b = 1$, with $b > 1.8$ for the best fit (lowest χ^2 contour) range. For a given value of b, the non-linear bias c_2 is slightly larger for the $\Omega h = 0.2$ case than for standard $\Omega h = 0.5$ CDM. For the CGF model, on the other hand, the linear bias parameter must satisfy $b > 2$ for a reasonable fit, while the best fit range requires $b > 3$. The large value of bias for the CGF model inferred from S_3 is qualitatively similar to the result above from the Fourier-amplitude Q_Δ: fits to the data with large values of b are in a sense *ad hoc*, because the agreement is obtained by depressing the gravitational contribution and then fitting with the non-linear bias c_2 alone. In particular, for $c_2/b \simeq 0.6$, the galaxy amplitude $S_{g,3} \simeq 2 \simeq 3Q$ is completely produced by non-linear bias, not by gravitational or cooperative effects. Therefore the fit for the CGF model, for which $c_2/b = 0.6$, does not really reflect agreement between the data and the CGF model, but rather the possibility that, in any model, the observed signal comes from the non-linear component of biasing.

At this point, it is worth noting several features of the S_3 observations. The skewness has been measured from other redshift and angular catalogs in addition to those used above; a useful compendium of results in the literature is given in Fry and Gaztañaga (1993b). Except for the Lick catalog, the values of S_3 inferred from other surveys are broadly consistent with those shown in Fig. 4 (e.g., Bouchet, etal. 1991, 1993, Meiksin, etal. 1992). A second issue concerns redshift distortions of the higher order

moments. It is well known that peculiar velocities distort the galaxy power spectrum (Kaiser 1987), so that the power measured in a redshift catalog does not precisely represent the clustering power in real space. The transformation from the real space to redshift space power spectrum depends on the ratio $\Omega^{0.6}/b$. The extent to which this affects higher moments has been somewhat controversial: in N-body simulations, Lahav etal. (1993) find that S_3 is significantly distorted in redshift space in the strongly non-linear regime, while Coles, etal. (1993) do not see this affect. In their analysis of higher moments in the CfA, SSRS, and IRAS 1.9 Jy catalogs, Fry and Gaztañaga (1993b) find that the volume-average 3-point function $\bar{\xi}_3$ is affected by redshift distortions, but that the normalized skewness S_3 is insensitive to them. This empirical insensitivity justifies our comparison of the model results to the S_3 data in redshift space.

We finish this section with some comments about the implications of the Q and S_3 observations for the bias parameter(s) and how these compare with other data on large-scale structure. We will focus on the CDM models (as opposed to the CGF model). First, as noted above, the Q_Δ observations do not significantly constrain the bias parameter b once one allows for non-linear bias (although they do imply a relation between b and c_2). On the other hand, the S_3 observations do appear to favor larger values of the bias, $b \gtrsim 1.8$, for both CDM models. In a simple bias prescription, for CfA galaxies we would expect $b\sigma_8 \sim 1$, so that, taken at face value, this constraint on b would imply a low normalization amplitude for the CDM models, $\sigma_8 \lesssim 0.56$. For standard $\Omega h = 0.5$ CDM, this is uncomfortably low compared to the amplitude inferred from the COBE DMR measurement of the large-angle microwave anisotropy, $\sigma_{8,dmr} \sim 1$. For the low-density CDM model, the σ_8 amplitude inferred from COBE has a large range, depending on the choice of Ω and h (Efstathiou, Bond, and White 1992). For example, for the choice $\Omega = 0.3$, $h = 2/3$, Efstathiou, Bond, and White (1992) infer $\sigma_8 \sim 0.7$ from COBE, closer to the range implied by the S_3 observations. (On the other hand, for lower Ω and larger h, e.g., $\Omega = 0.2$ and $h = 1$, the COBE value for σ_8 becomes larger than unity, which is disfavored by the 3-point data.) While it is tempting to draw conclusions about the viability of different models from this comparison, in particular, to argue against standard COBE-normalized CDM, there are potential pitfalls which mitigate against making high confidence-level statements of this type. In particular, if one focused only on the S_3 data in Fig.4 at large R (where the perturbation result is more trustworthy), one would conclude that standard $\Omega h = 0.5$ CDM fits the data well with $b \simeq 1$, $c_2 \sim 0$, in agreement with the COBE normalization. A conclusion which can be drawn with more confidence from Fig. 5 is that the high peaks model prediction $c_2/b = 1$ is inconsistent with the S_3 data for any of the Gaussian models we have studied.

6 Conclusion

We have studied the three-point galaxy correlations in models of large-scale structure, focusing on the CDM model and its variants with extra large-scale power, working in the context of biased galaxy formation in second order perturbation theory. In the non-local bias scheme, galaxies form and light up in just such a way as to create the illusion of extra power. We have shown that models with effective

scale-dependent (or non-local) bias, such as the CGF model, can display the same enhanced large-scale power as other variations of standard CDM, but that they break the scaling hierarchy between the two- and three-point functions that arises from gravitational evolution. The resulting step in the Fourier-space three-point function $Q_\Delta(k)$ at the scale $k \sim R_s^{-1}$ of the bend in the bias function (which produces the extra large-scale power) should provide a strong observational test of scale-dependent bias models. However, this step can be partially masked if b is large and if there is significant non-linear bias. Consequently, using data currently available, we have shown that the scale-dependent bias explanation of large-scale power requires a larger value of the linear bias factor b than in the standard CDM model, and a substantial non-linear bias, in order to account for the observed flatness of the three-point amplitudes.

On the other hand, the three-point amplitudes S_3 and Q do not strongly discriminate between standard and low-density CDM with scale-independent bias; this conclusion also extends to the tilted CDM and mixed dark matter models. In these cases, however, the S_3 data tentatively point to moderately large values of the bias, $b \gtrsim 1.8$, but more data on large scales is needed to confirm this. We emphasize that it is useful to have observational tests using both S_3 and Q_Δ, since the former depends on the power spectrum while the latter does not.

For completeness, we note that the CGF and other non-local bias models have other hurdles to overcome in addition to the higher moments. In the CGF and related models, the effective bias factor increases with lengthscale. On the other hand, recent N-body simulations of CDM incorporating hydrodynamics suggest that the bias factor $b(k)$ *decreases* with lengthscale (Cf. Katz, Hernquist, and Weinberg 1992, Fig.2 of Cen and Ostriker 1992). In addition, the modifications introduced by CGF do not apparently address the difficulties which CDM faces with excessive pairwise velocities on small scales (Gelb and Bertschinger 1993 and references therein). On the other hand, it would be interesting to study whether there might be a cooperative analogue for velocity bias (Couchman and Carlberg 1992).

Acknowledgements

Figure Captions

Fig. 1. The two-point spatial correlation function $\xi(r)/(b\sigma_8)^2$ in linear theory for standard CDM ($\Omega h = 0.5$), low-density CDM ($\Omega h = 0.2$), and CGF-modified standard CDM with $\kappa = 2.29$, $R_s = 20\,h^{-1}$ Mpc.

Fig. 2. The volume-averaged normalized skewness $S_3(R)$ in second-order theory is shown as a function of top-hat smoothing radius R for the three models of Fig. 1.

Fig. 3. The Fourier-space 3-point amplitude for equilateral triangles $Q_\Delta(k)$ is shown as a function of wavenumber k. The data points (from Baumgart and Fry 1991) are an average over subsamples from the CfA and Perseus-Pisces surveys. The model points are for standard perturbation theory (short dashed line, $Q_\Delta = 4/7$), and for the three CGF models discussed by BCFW: $\kappa, R_s = 0.84, 10\,h^{-1}$ Mpc (dot-long dash), $2.29, 20\,h^{-1}$ Mpc (solid), and $4.48, 30\,h^{-1}$ Mpc (dot-short dash). For the models, we have taken $b = 1$, $c_2 = 0$.

Fig. 4. The volume-average skewness $S_3(R)$ for the same models as in Fig. 2 are shown in comparison with data from the CfA and SSRS surveys (from Gaztañaga 1992). The models are shown with $b = 1$, $c_2 = 0$.

Fig. 5. Contours of $\chi^2 = 5$, 8, and 14 (for 9 degrees of freedom) in the $b - c_2$ parameter space for fits of the 3 models to the data in Fig. 4. The darker regions correspond to lower χ^2. (a) CDM $\Omega h = 0.5$, (b) CDM $\Omega h = 0.2$, (c) CGF $\kappa = 2.29$, $R_s = 20\,h^{-1}$ Mpc.
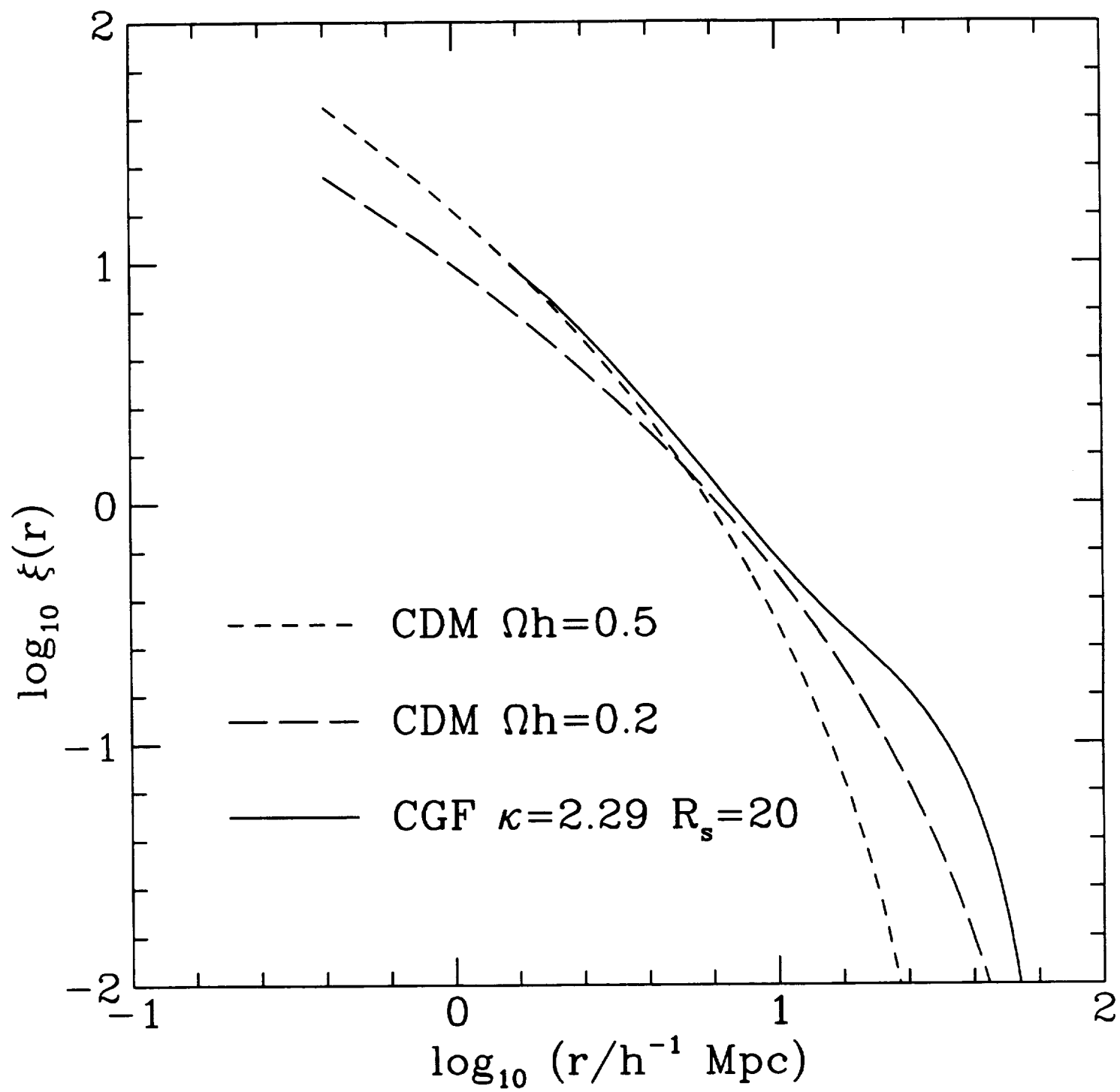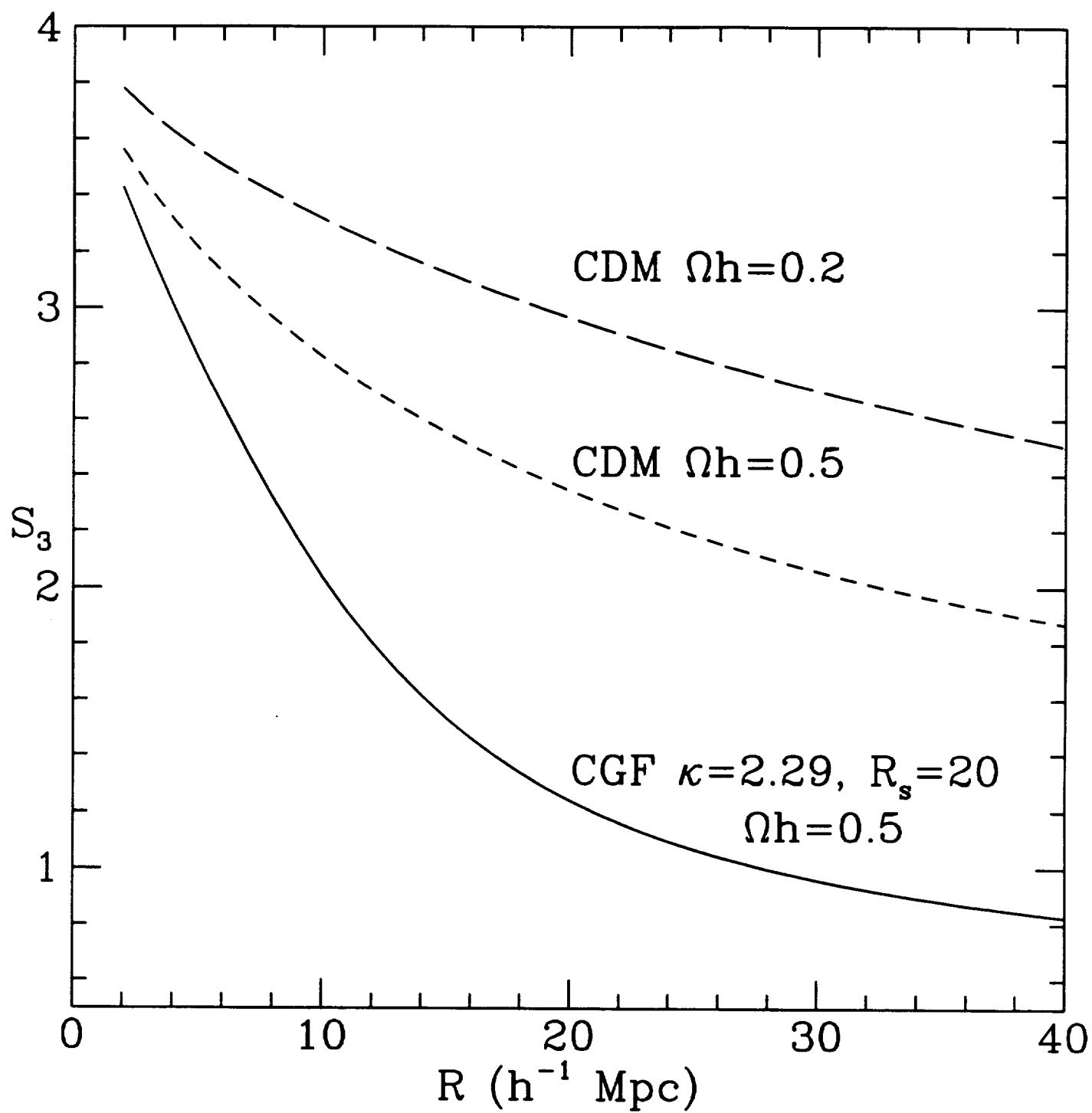
References

Adams, F. C., Bond, J. R., Freese, K., Frieman, J. A., & Olinto, A. V. 1993, Phys.Rev.D, 47, 426

Bardeen, J. M., Bond, J. R., Kaiser, N., & Szalay, A. S. 1986, ApJ, 304, 15

Babul, A., & White, S. D. M. 1991, MNRAS, 253, 31P

Bardeen, J. 1984, in *Inner Space/Outer Space*, eds. E. Kolb, M. Turner, D. Lindley, K. Olive, and D. Seckel, (Chicago:Univ. of Chicago press, 1986)

Baumgart, D. J., & Fry, J. N. 1991, ApJ, 375, 25

Bernardeau, F. 1992, ApJ, 392, 1

Bower, R., Coles, P., Frenk, C.S., & White, S.D.M. 1993, ApJ;405;403

Bouchet, F. R., Strauss, M., Davis, M., Fisher, K., Yahil, A., & Huchra, J. 1993, preprint

Bouchet, F. R., Davis, M., & Strauss M. 1991, in *The Distribution of Matter in the Universe*, eds. G. Mamon & D. Gerbal (Meudon: Observatoire de Paris)

Bouchet, F. R. & Hernquist, L. 1992, ApJ, 400, 25

Couchman, H. M. P. & Carlberg, R. 1992, ApJ, 389, 453

Cen, R., Gnedin, N. Y., Kofman, L. A., & Ostriker, J. P. 1993, ApJ, 399, L11

Cen, R., & Ostriker, J. P. 1992, ApJ, 399, L113

Coles, P., Moscardini, L., Lucchin, F., Matarrese, S., & Messina, A. 1993, preprint

Da Costa, L. N., Pellegrini, P., Davis, M., Meiksin, A., Sargent, W., & Tonry, J. 1991, ApJS, 75, 935

Davis, M., Summers, F. J., & Schlegel, D. 1992, Nature, 359, 393

Dekel, A., & Rees, M. J. 1987, Nature, 326, 455

Efstathiou, G., Bond, J. R., & White, S. D. M. 1992, MNRAS, 258, 1P

Efstathiou, G., Kaiser, N., Saunders, W., Lawrence, A., Rowan-Robinson, M., Ellis, R. S., & Frenk, C. S. 1990, MNRAS, 247, 10P

Efstathiou, G., Sutherland, W., & Maddox, S. J. 1990, Nature, 348, 705

Feldman, H., Kaiser, N., & Peacock, J. 1993, preprint UM AC 93-5

Fisher, K. B., Davis, M., Strauss, M. A., Yahil, A., & Huchra, J. P. 1993, ApJ, 402, 42

Fry, J. N. 1984, ApJ, 279, 499

Fry, J. N. 1985, ApJ, 289, 10

Fry, J. N. 1986, ApJ, 308, L71

Fry, J.N. & Gaztañaga, E. 1993a, ApJ in press (FERMILAB-Pub-92/367-A)

Fry, J.N. & Gaztañaga, E. 1993b, preprint FERMILAB-Pub-93/097-A

Fry, J. N. & Seldner, M. 1982, ApJ, 259, 474

Gaztañaga, E. 1992, ApJ, 398, L17

Gelb, J., and Bertschinger, E. 1993, preprint FERMILAB-Pub-92/74-A

Gelb, J., Gradwohl, B., & Frieman, J. A. 1993, ApJ, 403, L5

Goroff, M. H., Grinstein, B., Rey, S. J., & Wise, M. B. 1986, ApJ, 311, 6
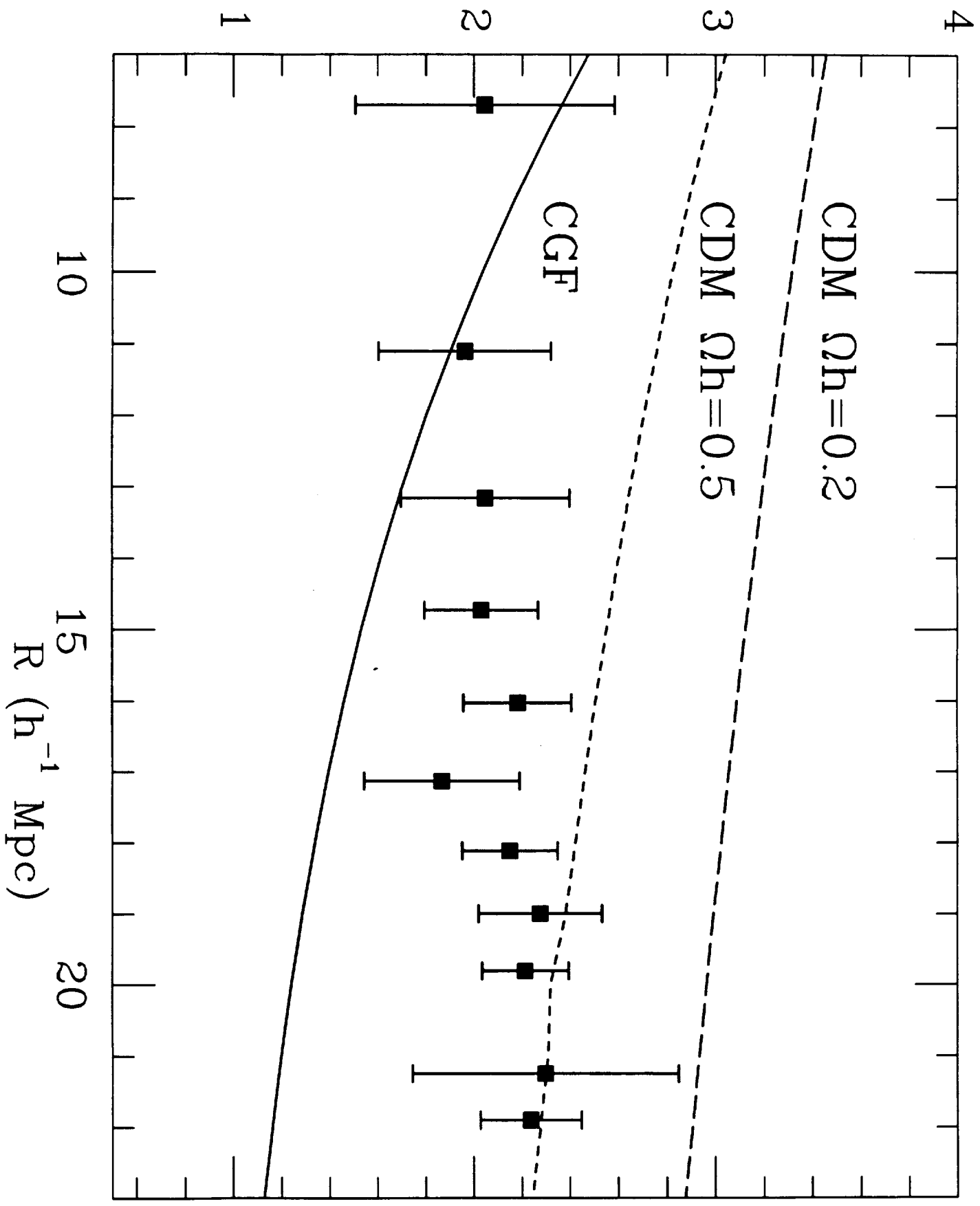
Gramann, M., & Einasto, J. 1991, MNRAS, 254, 453

Groth, E. J. & Peebles, P. J. E. 1977, ApJ, 217, 385

Hamilton, A. J. S. 1988, ApJ, 332, 67

Hamilton, A. J. S., Kumar, P., Lu, E., & Matthews, A. 1991, ApJ, 374, L1

Haynes, M., & Giovanelli, R. 1988, in *Large-Scale Motions in the Universe*, ed. V. C. Rubin & G. V. Coyne (Princeton: Princeton University Press)

Huchra, J., Davis, M., Latham, D., & Tonry, J. 1983, ApJS, 52, 89

Juszkiewicz, R., & Bouchet, F. 1991, in *The Distribution of Matter in the Universe*, eds. G. Mamon & D. Gerbal (Meudon: Observatoire de Paris)

Kaiser, N. 1984a, ApJ, 284, L9

Kaiser, N. 1984b, in *Inner Space/Outer Space*, eds. E. Kolb, M. Turner, D. Lindley, K. Olive, and D. Seckel, (Chicago: University of Chicago press, 1986)

Kaiser, N. 1987, MNRAS, 227, 1

Katz, N., Hernquist, L., & Weinberg, D. H. 1992, ApJ, 399, L109

Katz, N., Quinn, P., & Gelb, J. 1992, preprint

Lahav, O., Itoh, M., Inagaki, S., & Suto, Y. 1993, ApJ, 402, 387

Klypin, A., Holtman, J., Primack, J., & Regos, E. 1992, preprint

Liddle, A., & Lyth, D. H. 1992, preprint

Liddle, A., Lyth, D. H., & Sutherland, W. 1992, Phys.Lett.B, 279, 244

Loveday, J., Efstathiou, G., Peterson, B. A., & Maddox, S. J. 1992, ApJ, 400, L43

Maddox, S. J., Efstathiou, G., Sutherland, W. J., & Loveday, J. 1990, MNRAS, 242, 43P

Meiksin, A., Szapudi, I., & Szalay, A. S. 1992, ApJ, 394, 87

Moscardini, L., Borgani, S., Coles, P., Lucchin, F., Matarrese, S., Messina, A., & Plionis, M. 1993, preprint

Park, C., Gott, J. R., & da Costa, L. N. 1992, ApJ, 392, L51

Peacock, J. A., & Nicholson, D. 1991, MNRAS, 253, 307

Peebles, P. J. E. 1980, *The Large Scale Structure of the Universe*, (Princeton: Princeton University press)

Pogosyan, D., & Starobinsky, A. 1992, preprint

Politzer, H. D., & Wise, M. B. 1984, ApJ, 285, L1

Rees, M. J. 1985, MNRAS, 213, 75P

Saunders, W., etal. 1991, Nature, 349, 32

Schaefer, R. K., Shafi, Q., & Stecker, F. 1989, ApJ, 347, 575

Silk, J. 1985, ApJ, 297, 1

Szalay, A. S. 1988, ApJ, 333, 21

Szapudi, I., Szalay, A. S., & Boschan, P. 1992, ApJ, 390, 350

Taylor, A. N., & Rowan-Robinson, M. 1992, Nature, 359, 396

van Dalen, A., & Schaefer, R. K. 1992, ApJ, 398, 33

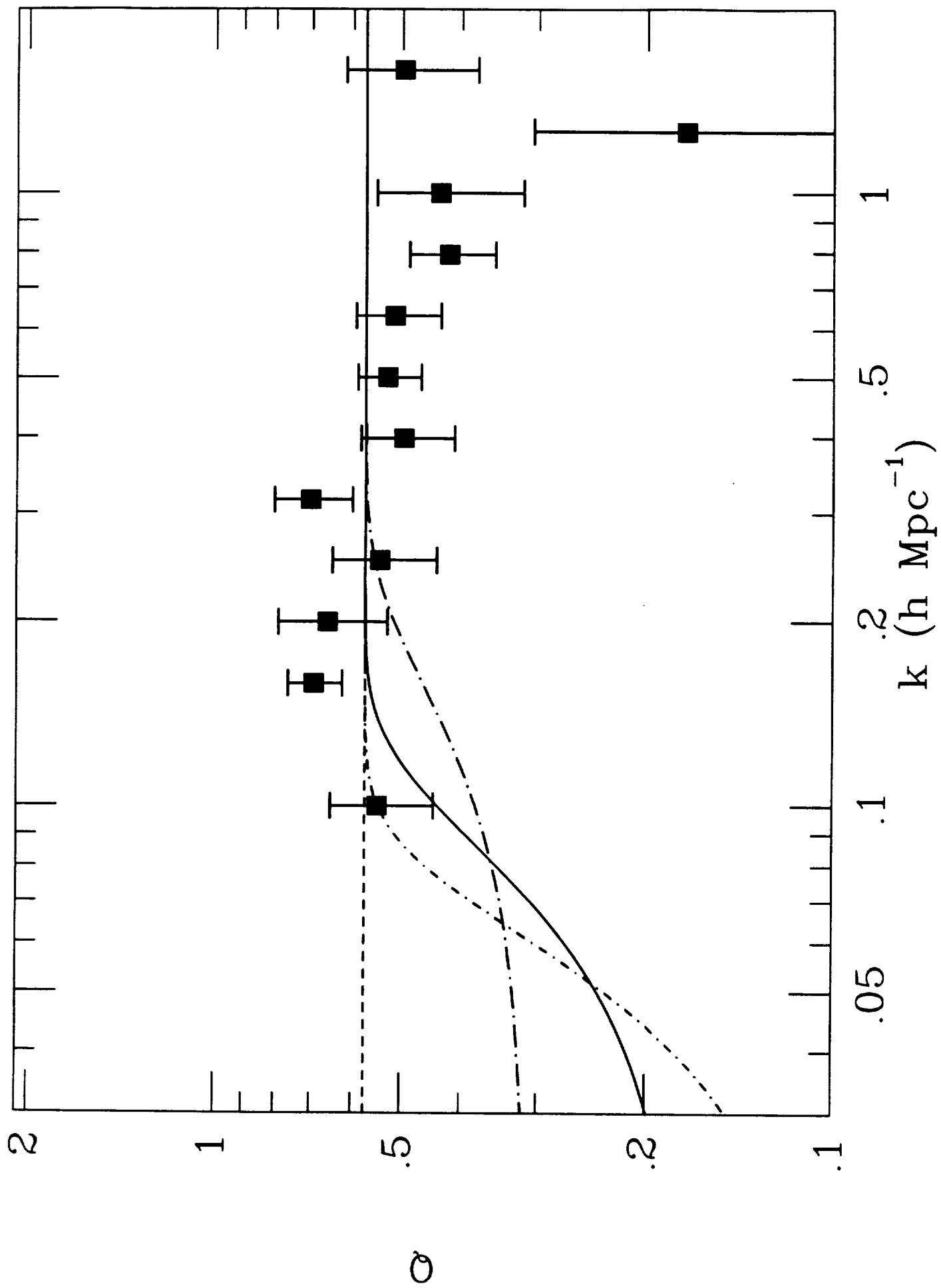Vittorio, N., Mattarese, S., & Lucchin, F. 1988, ApJ, 328, 69

Vogeley, M. S., Park, C., Geller, M. J., & Huchra, J. P. 1992, ApJ, 395, L5

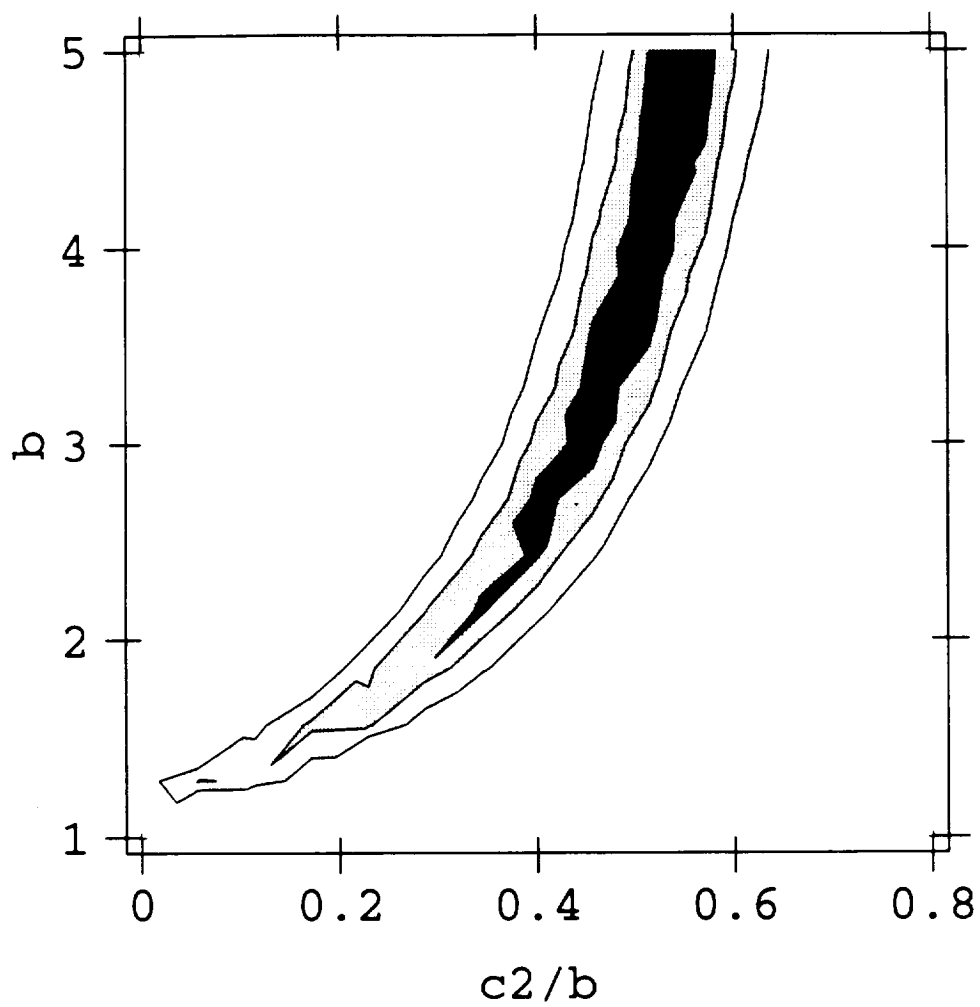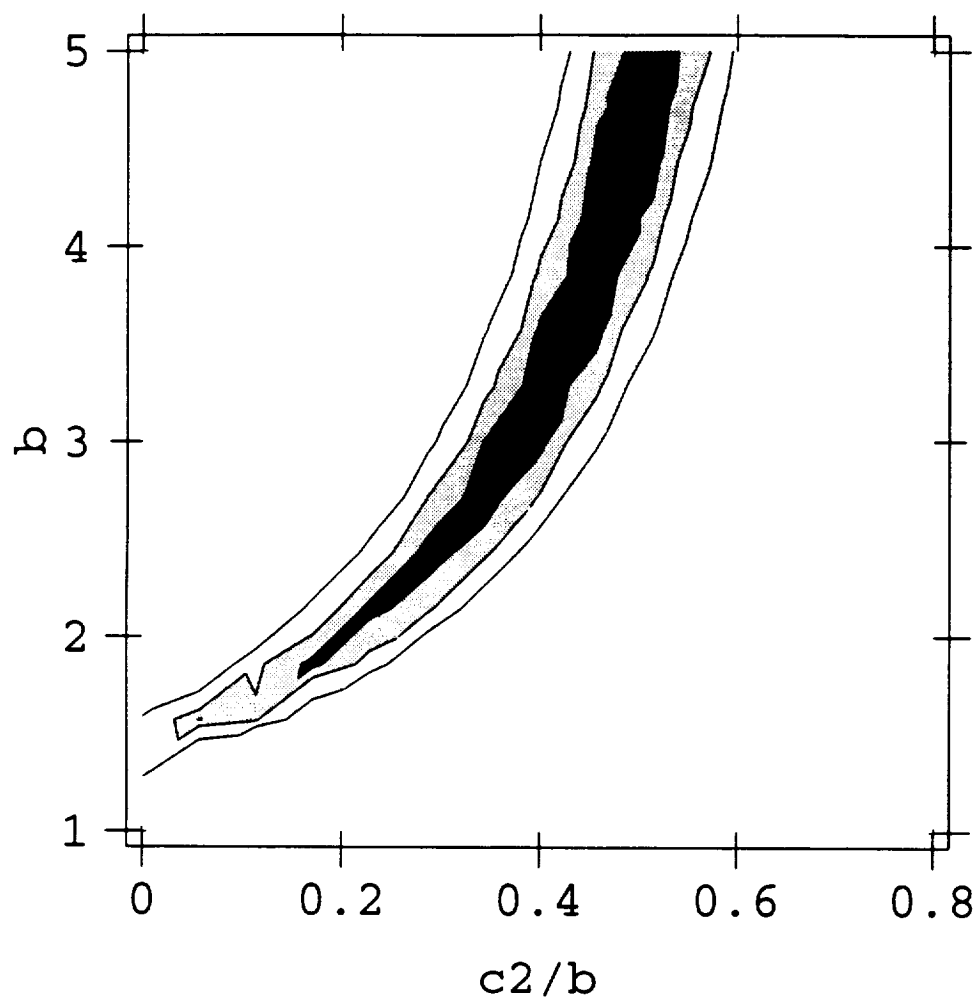White, S. D. M., Davis, M., Efstathiou, G., & Frenk, C. S. 1987, Nature, 330, 451

CDM, $\Omega h = 0.5$

CDM, $\Omega h = 0.2$

CGF